Performance Analysis of Adaptive GPS Signal Detection in Urban Interference Environment using the Monte Carlo Approach

V. Behar[1], Ch. Kabakchiev[2], I. Garvanov[3] and H. Rohling[4]
[1]Institute of Information and Communication Technologies-BAS,
[2]Sofia University "Sv. Kl Ohridski",
[3]State University of Library Studies and Information Technologies,
[4]Technical University Hamburg-Harburg,
[1,2,3]Bulgaria
[4]Germany

1. Introduction

The Global Positioning System (GPS) has been designed to provide precision location estimates for various military and civil applications. Each of satellites transmits digitally coded data, and GPS receivers demodulate these signals from four or more satellites simultaneously in order to generate three time-difference-of–arrival estimates, allowing the user to measure the range to three satellites, and, as a result, to determine his position. Since a direct sequence spread spectrum (DSSS) signal is used in transmission, relatively low powers can be transmitted by the satellites and still to have adequate signal-to-noise ratio (SNR) for accurate position estimation. In fact, these signals have SNR of between -15dB and -30dB. In civil applications, therefore, the key to achieve the precise position estimation performance is the processing of very weak DSSS signals from satellites that contain coarse acquisition (C/A) digitally coded data. In order to extract the information from a GPS signal, the presence of the coarse acquisition (C/A) code must be detected in the signal arriving at the input of a GPS receiver. In each channel of a GPS receiver, the algorithm for detection of the C/A code that identifies the corresponding satellite is carried out by cross-correlation and thresholding procedures. The objective of the detection algorithm is to search for the presence of the GPS signal over a frequency range that covers every possible expected Doppler frequency. The intensity maximum in the time discrete n and the frequency bin m gives the beginning point of the C/A code in 200 ns resolution and the carrier frequency in 1 kHz resolution if the signal maximum is above the predetermined threshold of detection. Once the GPS signal is found, two important parameters, the beginning point of the C/A code period and the carrier frequency of the input signal, are measured. Next this information is passed on to the tracking algorithm in order to extract the navigation data (Tsui, 2005).

Whatever GPS signals have some degree of antijamming protection built into the signal structure itself, the weak signal strength of the received signal makes it easy for strong broadband interference to overcome the antijamming protection of the C/A code signal

(Sklar, 2003). If a strong broadband jamming source is nearby, the receiver noise may rise to the level where the SNR at the correlator output is below the threshold value required for tracking. In that case the capability of the correlator to detect the C/A code is very seriously degraded. Multipath is the other limiting factor in many GPS applications that affects pseudorange and carrier phase estimates. Signal multipath is the phenomenon where a satellite signal arrives at the receiver antenna after being reflected from different surfaces or buildings (Soubielle et al., 2002).

Various approaches can be used to mitigate GPS interference before signal processing in a GPS receiver (Fu et al., 2003; Sklar, 2003). One of them is to use different beamforming techniques for broadband nulling having in mind that the satellite signals and interfering signals usually originate from different spatial locations. The conventional (delay-and-sum) beamforming procedure is performed by the simplest non-adaptive algorithm, in which all weights have equal magnitudes and the phases are selected to steer the array in particular direction (Van Trees, 2002). Such a beamformer has unity response in each look direction, and in conditions of no directional interferences, the beamformer provides maximum SNR but it is not effective in the presence of directional jamming signals, intentional or unintentional. The other beamformers such as a Minimum Variance Distortionless Response (MVDR) beamformer can overcome this problem by suppressing interfering signals from off-axis directions (Vouras & Freburger, 2008; Tummonery, 2005). To suppress jamming signals, the MDVR beamformer does not require a priori information about them but only the information for the direction-of-arrival of a desired signal. The capability of the MVDR beamformer to improve the detectability of radar targets in conditions of strong jamming is invesigated in (Behar & Kabakchiev, 2009; Behar et al, 2010). The impact of different factors on the capability of the adaptive MVDR beamformer to mitigate broadband interference at the input of GPS receivers is studied in (Behar et al., 2009; Behar et al., 2010). FPGA implementation of the MVDR QR-based beamformer for broadband interference suppression in satellite navigation receivers is proposed in (Ganchosov, 2009). The performance of each beamforming method can be applied to different antenna array configurations. The antenna elements are put together in a known geometry, which is usually uniform - Uniform Linear Arrays (ULA), Uniform Rectangular Arrays (URA) or Uniform Circular Arrays (UCA) (Ioannides & Balanis, 2005; Moelker, 1996). Two configurations, URA and UCA, with the elements extended in two dimensions enable to control the beam pattern in both azimuth and elevation, and for that reason they can be used for implementation of beamforming in GPS receivers. The smallest inter-element spacing in antenna arrays is usually equal to or slightly less than half a wavelength of the satellite carrier frequency ($\lambda/2$) in order to avoid the problem of "spatial under-sampling". However, an interelement spacing smaller than $\lambda/2$ increases the risk of mutual coupling between antenna elements.

As a rule, the standard C/A code detection performance is designed having in mind the detection on the background of a receiver noise only (Tsui, 2005). However, the application of modern radar approaches to signal processing in a GPS receiver can overcome the problem associated with detection of weak GPS signals in conditions of strong urban interference. In this chapter we present our original idea to combine three different approaches in a new three-stage algorithm for detection of the C/A code in heavy urban noise environment (GPS MDVR CFAR). The proposed GPS MDVR CFAR detection algorithm includes three processing stages: (i) - adaptive Minimum Variance Distortionless Response (MVDR) beamforming algorithm applied to the software GPS receiver input; (ii) -

circular cross-correlation algorithm performed in the frequency domain; (iii) - CFAR signal thresholding algorithm applied to the cross-correlator output for maintaining the constant probability of false alarm. The design of the GPS MDVR CFAR detection algorithm is based on our experience in the research of algorithms for broadband/ pulse jamming suppression (Behar & Kabakchiev, 2009; Behar et al., 2010, Behar et al., 2009; Ganchosov et al., 2009) and target detection (Behar et al., 2000; Garvanov et al., 2003; Kabakchiev et al., 2010; Behar et al., 2010) in GPS and radar applications. In this chapter, the effectiveness of the GPS MDVR CFAR detection algorithm is expressed in terms of three quality parameters: the signal-to-noise-plus-interference ratio (SINR) improvement factor statistically estimated at the beamformer output; the post correlation signal-to-noise ratio (SNR) statistically estimated at the cross-correlator output and, finally, the probability of detection estimated at the CFAR detector output.

The three quality parameters of the GPS MDVR CFAR detection algorithm are evaluated using the Monte Carlo approach. The statistical estimates of the corresponding quality factors are evaluated for each stage of the detection algorithm. The objectives of the Monte Carlo analysis are: (i)- to analyze the capability of two beamformers, non-adaptive (conventional) and adaptive (MVDR), to mitigate broadband radio frequency interference (RFI) at the navigation receiver input and as a result to improve the post correlation SNR and, thus, increasing the probability of detection of the C/A code in conditions of strong jamming; (ii) - to evaluate the influence of several important factors on the performance of the joint three-stage detection algorithm. These factors include: interference intensity expressed in terms of the interference-to-signal ratio (ISR); planar array configuration (*URA* and *UCA*); number of array elements; sampling rate of the incoming data; angular errors in satellite location known as steering vector mismatch; reference window length used in a CFAR detector.

2. Antenna array geometry

Antenna arrays are composed of many antenna elements in order to create a unique radiation pattern in the desired direction. The antenna elements are put together in a known geometrical structure with uniform interelement spacing - Uniform Linear Arrays (ULA), Uniform Rectangular Arrays (URA) or Uniform Circular Arrays (UCA) (Van Trees, 2002; Ioannidis & Balanis, 2005). Since a ULA beam pattern can be controlled in only one dimension (azimuth), in GPS applications, only URA or UCA configurations with the elements extended in two dimensions should be used in order to control the beam pattern in two angular dimensions (azimuth and elevation).

2.1 URA configuration

In URA antenna arrays, all elements are extended in the *x-y* plane. There are M_X elements in the *x*-direction and M_Y elements in the *y*-direction creating an array of (M_X x M_Y) elements. All elements are uniformly spaced *d* apart in both directions. Such a rectangular array can be viewed as M_Y uniform linear arrays of M_X elements or M_X uniform linear arrays of M_Y elements. Usually, the first antenna array element is considered as the origin of Cartesian coordinates in (Fig. 1). The direction of a signal arriving from azimuth φ and elevation θ can be described with a unit vector *e* in Cartesian coordinates as:

$$e(\varphi,\theta) = (e_x, e_y, e_z) = (\cos\theta\sin\varphi, \cos\theta\cos\varphi, \sin\theta) \tag{1}$$

The element number $m(i,k)$ of an antenna array is calculated as:

$$m(i,k) = (i-1)M_X + k, \quad i = 1 \div M_Y , \ k = 1 \div M_X \tag{2}$$

The vector in the direction of element $m(i,k)$ can be described in Cartesian coordinates as:

$$r_{m(i,k)} = (d(i-1), d(k-1), 0) \tag{3}$$

In (3), indexes i and k denote the element position along the y- and the x-axis, respectively.
If the first element of a rectangular array is a reference element, the path-length difference $d_{m(i,k)}$ for a signal incident at element $m(i,k)$ can be defined as a projection of the vector $r_{m(i,k)}$ on the signal direction vector e:

$$d_{m(i,k)} = e^T \cdot r_{m(i,k)} = \cos\theta \cdot d \cdot [\sin\varphi(i-1) + \cos\varphi(k-1)] \tag{4}$$

Therefore, the URA response vector a_c in the direction (φ, θ) takes the form:

$$a_c(\varphi, \theta) = [1, \exp(j\frac{2\pi}{\lambda}d_2), \ldots, \exp(j\frac{2\pi}{\lambda}d_{m(i,k)}), \ldots, \exp(j\frac{2\pi}{\lambda}d_M)] \tag{5}$$

where $M = M_X \times M_Y$.

2.2 UCA configuration

In UCA antenna arrays, all elements are arranged along the ring of radius r (Fig. 2). The ring contains M array elements. Since these elements are uniformly spaced along the ring, they have an interelement angular spacing $\Delta\varphi = 2\pi/M$ and a linear interelement spacing $d = 2r\pi/M$. It is usually assumed that the first antenna element is located on the y-axis, and the ring center is the origin of Cartesian coordinates. The vector in the direction of the mth array element can be defined in Cartesian coordinates as:

$$r_m = (r\sin\varphi_m, r\cos\varphi_m, 0) , \text{ where } \varphi_m = 2\pi(m-1)/M \tag{6}$$

The unit vector $e(\varphi, \theta)$ in the direction of a signal source is given by (1). If the ring center serves as a reference point, the propagation path-length difference d_m for a signal incident at element m can be defined as a projection of the vector r_m on the direction vector e:

$$d_m = e^T \cdot r_m = d \cdot \cos\theta(\sin\varphi\sin\varphi_m + \cos\varphi\cos\varphi_m) = d\cos\theta\cos(\varphi - \varphi_m) \tag{7}$$

Therefore, the UCA response vector a_c takes the form:

$$a_c(\varphi, \theta) = [\exp(j\frac{2\pi}{\lambda}d_1), \exp(j\frac{2\pi}{\lambda}d_2), \ldots, \exp(j\frac{2\pi}{\lambda}d_m), \ldots, \exp(j\frac{2\pi}{\lambda}d_M)] \tag{8}$$

where d_m is expressed by (7) for $m=1,2,\ldots M$.
The vectors a_c in (5 and 8) are often called steering vectors that describe the array response to a signal arriving from direction (φ, θ).
The special case of a circular antenna array is a 7-element antenna array, where the first element is located in the antenna array centre, and the other six elements are arranged in a circle relative to the first element (UCA-7).
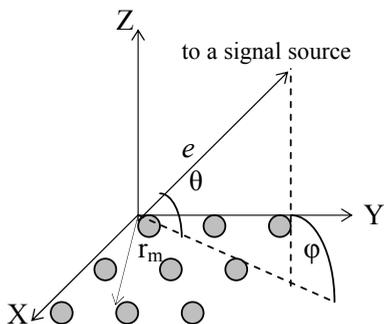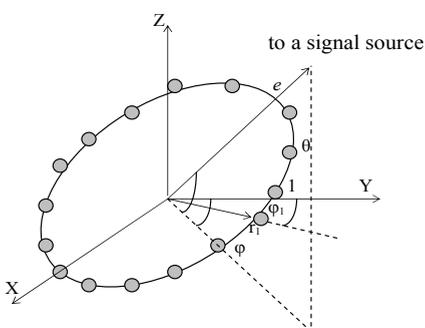
Fig. 1. URA configuration

Fig. 2. UCA configuration

3. Software-based GPS receiver

The structure of a software-based GPS receiver is shown in Fig. 3. The GPS receiver processes signals received from satellites that are in view, and then uses the extracted information to determine and display the user position, velocity, and time (Tsui, 2005).
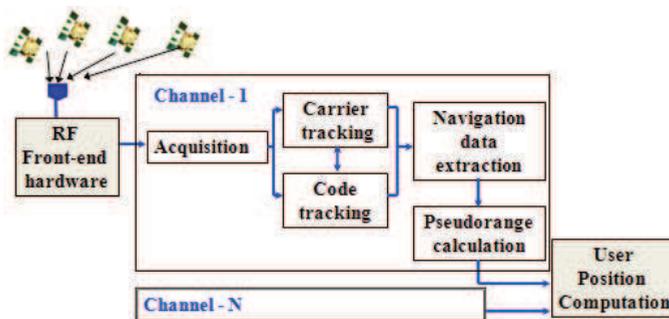
Fig. 3. Architecture of a software-based GPS receiver

The GPS receiver is a multi-channel device, where one channel processes the incoming signal from one satellite. The first two blocks of a GPS receiver are an antenna and a RF

front-end section that includes several devices, which are usually implemented in hardware. In the RF front-end section, the incoming signal is down converted from the RF frequency to an intermediate frequency (IF) in several stages. The down converters reduce the carrier frequency from GHz to a couple MHz. The last stage of the RF front-end section is an Analog-to Digital Converter (ADC), where the IF signals are sampled at a suitable sampling frequency and digitized. In the next blocks of the GPS receiver, the incoming signal is processed in multiple (from 8 to 12) parallel channels, where each channel acquires and dynamically tracks signals from one visible satellite.

As shown in Fig. 3, in each channel the acquisition block detects the signal of a certain satellite, then the tracking block is used to find the phase transition of the navigation data, and the navigation data is obtained from the navigation data phase transition. Further, the ephemeris data and pseudoranges are calculated from the navigation data. The ephemeris data is used to calculate the satellite position and, finally, the user position is obtained from the satellite position and the pseudoranges. Minimum four channels for tracking the signals of four satellites are required to determine three position coordinates and the receiver clock offset.

In a conventional hardware-based receiver, the acquisition and tracking blocks are implemented in an IC chip, and the algorithms implemented in the chip are not available for the user. In a software-based GPS receiver, however, these blocks are implemented in software and hence the user has a free access to these algorithms and can update them and exercise control over them. This is the difference between the software-based GPS receiver and a conventional hardware-based GPS receiver.

4. Signal model

GPS signals are transmitted at two radio frequency bands - L1 (1572.42 MHz) and L2 (1227.6 MHz). Each satellite transmits two unique codes. The first of them is the coarse acquisition code (C/A), and the second code is the encrypted precision code (P(Y)). The signal transmitted at L1 frequency contains the coarse acquisition (C/A) code, precision (P) code and navigation data while the signal transmitted at L2 frequency contains P-code only. We limit our discussion within the signal transmitted at L1 frequency that contains the C/A code only because the signal transmitted at frequency L2 and containing P-code serves for military purposes only and the civilian community does not have a free access to P-code. The C/A code modulated signal is a BPSK modulated signal. The null-to-null frequency bandwidth of the main lobe of this signal spectrum is 2.046 MHz. The total code period contains 1023 chips, and 1023 chips last 1ms with a chip rate of 1.023 MHz. The GPS C/A coded signals belong to the family of Gold codes, and they are unique for every satellite. The main property of the C/A code is that it has the best cross-correlation characteristic. The C/A code modulated signal transmitted by each satellite is the product of three signals: (i)-the carrier signal with frequency L1; (ii)-the navigation data with a bit rate of 50bps; (iii)-the C/A code that is unique for each satellite.

The signal received by an antenna array of a GPS receiver is composed of the satellite signal, thermal noise and a variety of interference. In conditions of jamming, the complex valued samples of the received signal at time instant k can be mathematically described as:

$$x(k) = a_c s(k) + \sum_{l=1}^{L} b_l j_l(k) + n(k) \tag{9}$$

where $x(k)$ is the $(M \times 1)$-element signal vector, $s(k)$ is the received satellite signal sample, $j_l(k)$ is the lth broadband jamming sample, a_c and b_l are the $(M \times 1)$-element antenna array response vectors in the direction of a satellite signal and the lth broadband interference, respectively, $n(k)$ is the noise sample and L is the number of broadband interference sources. The signal received from a satellite can be described as:

$$s(k) = \sqrt{SNR} \cdot c(k) \cdot \cos(2\pi f_0 t_k + \varphi) \cdot d(k) \qquad (10)$$

where SNR is the received signal-to-noise ratio, $c(k)$ is the C/A code of length (20×1023), unique for each satellite, $d(k)$ is the navigation data bit which remains constant over 20 periods of the C/A code, and f_0 is the carrier intermediate frequency. The jamming signal $j(k)$ occupies the entire receiver bandwidth and can be modelled as bandlimited additive white Gaussian noise (AWGN) with zero mean:

$$j(k) = \sqrt{INR} \cdot N(0,1) \qquad (11)$$

where INR is the interference-to-noise ratio. The noise sample $n(k)$ can be modeled as additive white Gaussian noise with zero mean and unity variance. In GPS applications, when the receiver is on the ground, the input SNR value depends on the RF-bandwidth of the receiver front-end and is typically around -20dB (2.046 MHz C/A code bandwidth).

5. GPS signal detection

As a rule, the standard C/A code detection performance is designed having in mind the signal detection on the background of a receiver noise only (Tsui, 2005). However, the application of modern radar approaches to signal processing in a GPS receiver can overcome the problems associated with detection of weak GPS signals in conditions of strong urban interference. In this section we present our original idea to combine three different approaches in a new three-stage algorithm for detection of the C/A code in heavy urban noise environment (GPS MDVR CFAR) (Fig.4).
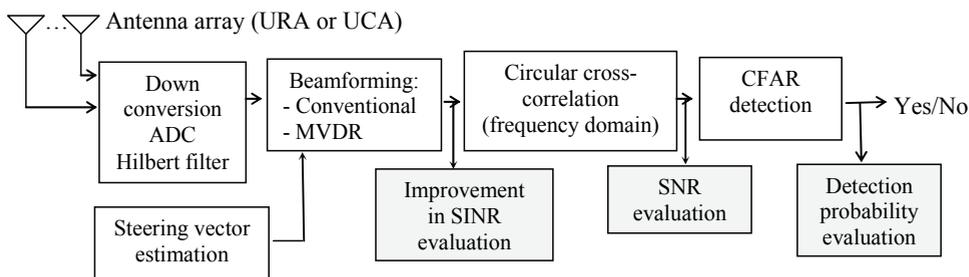

Fig. 4. Flow-chart of the signal processing and the evaluation process

As shown in Fig.4, in the RF front-end section of each antenna element, the GPS signal is down converted from the RF frequency to an intermediate frequency (IF), sampled at a suitable sampling frequency and digitized. After Hilbert filtration the signal is converted into complex form. The complex-valued signal is then performed by the new GPS MDVR CFAR detection algorithm that includes three processing blocks. The first of them is a

beamformer that mitigates broadband interference before detection of the C/A code. The beamformer can be realized as a non-adaptive block, where the conventional "delay-and-sum" method is implemented, or as an adaptive one, where some adaptive method is implemented - for example, the Minimum Variance Distortionless Response (MVDR) method. In the second block the circular cross-correlation procedure is performed in the frequency domain. The incoming signal is correlated with the local signal replica in order to identify the visible satellite in the incoming data and then find the beginning point of the C/A code and estimate the rough Doppler shift. The third block is used to detect the presence of the C/A code at the cross-correlator output while maintaining the constant probability of false alarm. The performance of the modified Cell Averaging CFAR (CA CFAR) detector is considered to be used in this block.

5.1 Beamforming methods

The digital beamformer increases the gain in the direction of arrival of the desired signal, and decreases the gain in all other directions (interference). For an antenna array composed of M elements, the output signal Y is formed as a weighted sum of signals X arrived at the antenna input (Fig.5):

$$Y = W^H X ,$$ (12)

In (12), X is the input signal matrix of size (M x N), N is the number of time samples, W is the complex valued weight vector of size M, and $(.)^H$ denotes conjugate transpose.
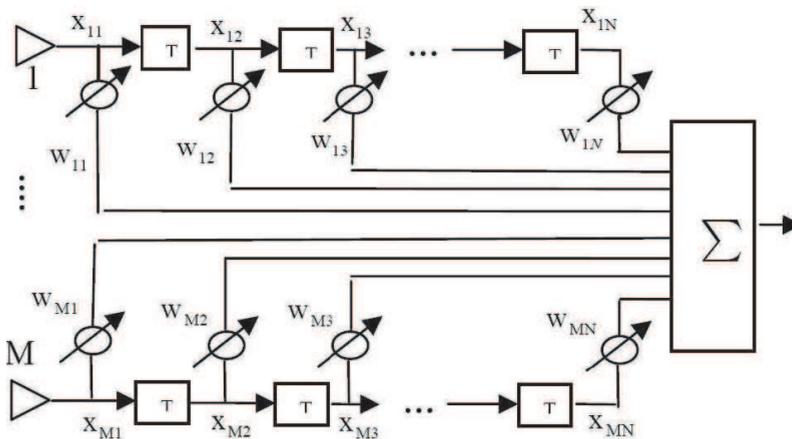

Fig. 5. Block diagram of the beamforming technique for GPS interference mitigation.

Conventional Beamformer: In a conventional beamformer, the complex vector of weights W is equal to the array response vector a_c, which is defined by an array configuration (Moelker, 1996):

$$W_{conv} = a_c$$ (13)

For URA and UCA configurations the array response vector a_c is calculated using (5) and (8), respectively.

MVDR Beamformer: In GPS applications, the objective of adaptive beamforming is to maximize the gain in the direction of arrival of the desired signal from GPS and mitigate broadband interference incoming from the other directions. The weight vector W can be chosen to maximize the signal-to-interference-plus-noise ratio at the antenna output (Tummonery, 1994):

$$SINR = \frac{\sigma_S^2 \left| W^H a_c \right|^2}{W^H K_{j+n} W}$$
(14)

where K_{j+n} is the "interference + noise" covariance matrix of size ($M \times M$), and σ_S^2 is the signal power. The easy solution of the optimization problem (14) can be found by maintaining the distortionless response toward the desired signal and minimizing the power at the beamformer output. This criterion of optimization is formulated as:

$$\min_{W} W^H K_{j+n} W \quad \text{to subject} \quad W^H a_c = 1$$
(15)

The solution of the optimization problem (15) is known as a minimum variance distortionless response beamformer (MVDR):

$$W_{MVDR} = \frac{K_{j+n}^{-1} a_c}{a_c^H K_{j+n}^{-1} a_c}$$
(16)

In practical applications, the covariance "interference plus noise" matrix K_{j+n}, is unavailable and the sample covariance matrix is used instead of it. The sample covariance matrix is estimated as:

$$\hat{K} = X^H X$$
(17)

Many practical applications of MVDR-beamformers require online calculation of the weights according to (16), and it means that the covariance matrix (17) should be estimated and inverted online. However, this operation is very computationally expensive and it may be difficult to estimate the sample covariance matrix in real time if the number of samples MN is large. Furthermore, the numerical calculation of the weights W_{MVDR} using the expression (16) may be very unstable if the sample covariance matrix is ill-conditioned. A numerically stable and computationally efficient algorithm can be obtained by using QR decomposition of the incoming signal matrix. The signal matrix is decomposed as $X=QR$, where Q is the unitary matrix and R is the upper triangular matrix. In that case the sample covariance matrix is calculated as:

$$\hat{K} = X^H X = (QR)^H (QR) = R^H R$$
(18)

Taking into account (18), the expression (16) takes the form:

$$W_{MVDR} = \frac{R(R^H)^{-1} a_c}{a_c^H R(R^H)^{-1} a_c}$$
(19)

In accordance with (19) the *QR*-based algorithm for calculation of beamformer weights includes the following three steps:

- The linear equation system $R^H z_1 = a_c$ is solved. The solution is $z_1^* = (R^H)^{-1} a_c$
- The linear equation system $R z_2 = z_1^*$ is solved. The solution is $z_2^* = R^{-1} z_1^*$
- The weight vector $\widehat{W}$ is obtained as $\widehat{W} = z_2^* / (a_c^H z_2^*)$

5.2 Circular cross-correlation

The main purpose of the cross-correlation stage is to identify the visible satellites in the incoming data and then find the beginning point of the C/A code and estimate the rough Doppler shift by correlating the incoming signal with the local signal replica. In a hardware-based GPS receiver, the conventional cross-correlation algorithm is implemented in hardware and the processing is performed in the time domain. In a software-based GPS receiver, the circular cross-correlation algorithm shown in Fig. 6 can be considered as a reduced computational version of the conventional cross-correlation method. In contrary to the conventional method the circular cross-correlation is performed in the frequency domain.
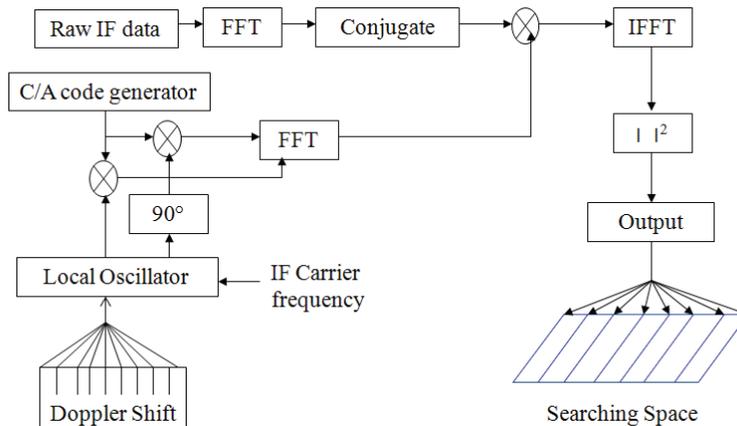

Fig. 6. Block diagram of the circular cross-correlation technique

At the circular cross-correlator output, the detection method should search over a frequency range of [-10KHz, 10KHz] to cover the expected Doppler frequency range for a high speed aircraft. This method is very suitable for software receiver implementation. The idea is that the input data sampled and stored in memory can be performed as blocks of data. Since the C/A code period is 1ms long, the circular cross-correlation must be performed on at least 1ms of the incoming data. According to (Tsui, 2005) the circular cross-correlation algorithm consists of the following steps:

- Perform the FFT of the input data $x(k)$ converting them into frequency domain as $X(k)$.
- Take the complex conjugate $X(k)$ obtaining the outputs $X^*(k)$.
- Generate 21 local codes $l_{si}(k)$ as $l_i(k) = c(k) exp(2\pi j f_i)$, , where $f_i = f_c + i \cdot$ kHz, f_c- is the intermediate frequency and i=-10,-9,….9, 10. The local code is the product of the C/A code of a satellite and a complex IF signal. The frequencies f_i of the local codes are separated by 1 kHz.

- Perform the FFT of the local codes $l_{si}(k)$ to transform them to the frequency domain as $L_i(k)$.
- Multiply $X^*(k)$ and $L_i(k)$ point by point obtaining the result $R_i(k)$.
- Take the IFFT of $R_i(k)$ to transform the result into time domain as $r_i(k)$.

5.3 CA CFAR detection

The constant false alarm rate (CFAR) signal detector is based on the principle of evaluating the noise power level to maintain the constant rate of false alarms (Finn & Johnson, 1968). The noise power estimate is calculated by integration of samples over a certain number of cells referred to as a reference window. The noise power estimate obtained is weighted with a scale factor to form an adaptive threshold, which is then compared to the signal from a cell under test. The structure of an adaptive Maximum Likelihood CFAR (ML CFAR) detector is shown in Fig. 7.
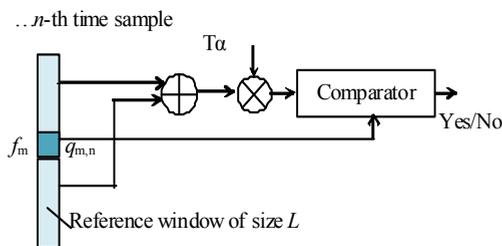
Fig. 7. Block diagram of the CFAR detector

In the ML CFAR detector, the decision rule for detection of the C/A code is formulated as:

$$\Phi_{m,n} = \begin{cases} 1, if\ q_{m,n} \geq T_a \cdot w_{m,n} \\ 0, \quad otherwise \end{cases} \quad (20)$$

According to (20), if the test statistics $q_{m,n}$ exceeds a threshold of detection $T\alpha \cdot w_{m,n}$, then the nth time discrete and the mth frequency bin give the beginning point (τ_{sat}) of the C/A code in $(1/f_s)$ resolution in the input data and the carrier frequency ($f_{c,sat}$) in 1kHz resolution:

$$f_{c,sat} = f_c + m \cdot 1KHz\ , \quad \tau_{sat} = n\ /\ f_s \quad (21)$$

The parameter f_s in (21) is the sampling frequency of the incoming IF data. The test statistics $q_{m,n}$ in (20) is formed as:

$$q_{m,n} = \max_{i,k}\{r_i^2(k)\}\ for\ i = m, k = n \quad (22)$$

The index i in (22) varies in the range of -10 to 10 and the index k varies from 1 to K, where K is the number of time samples of r_i on 1ms of data. The variable $w_{m,n}$ in (20) is the estimate of the total noise power integrated over a reference window of length L. It is calculated as:

$$w_{m,n} = \sum_{\substack{l=m-L/2 \\ l \neq m}}^{m+L/2} r_m^2(n) \quad (23)$$

Since the sort procedure used for finding $q_{m,n}$ in (22) is computationally expensive, we propose firstly to perform the thresholding over all the data in the search field with a single threshold and, secondly, to search the maximum only over the data that exceeded the threshold of detection. The decision rule of thresholding is formed as follows:

$$\Phi_{i,k} = \begin{cases} 1, if \; r_i^2(k) \geq T_a \cdot w \\ 0, \quad otherwise \end{cases} \tag{24}$$

In order to form a single threshold of detection ($T_a w$) in (24), we propose to use a reference window that includes L samples of r_i contained in four frequency bins, for example, $f_{-10}=f_c-10KHz; f_{-9}=f_c-9KHz; f_{10}=f_c+10KHz; f_9=f_c+9KHz$ (Fig. 8).
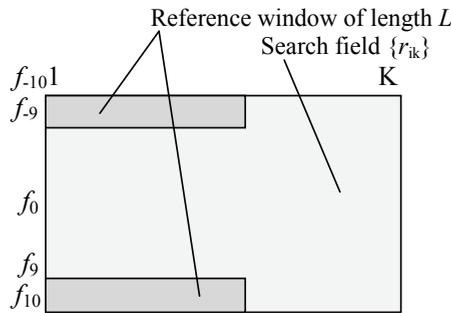
Fig. 8. Position of a reference window in the search field of data

In that case the noise power is estimated as:

$$w = \sum_{l=1}^{L/4} \{r_{-10}^2(l) + r_{-9}^2(l) + r_9^2(l) + r_{10}^2(l)\} \tag{25}$$

The time discrete n and the frequency bin m, which give the two C/A code parameters in (21), are determined as:

$$\{m,n\} = \arg\max\{r_i^2(k), \Phi_{i,k} = 1\} \tag{26}$$

The accuracy of the estimate w in (25) directly depends on the reference window length (L). The choice of L depends on whether the reference window contains the GPS signal or not. There are three possible ways of choosing the appropriate window length:

- to use a small reference window of length L free of a GPS signal, which is enough to obtain the accurate estimate w;
- to use a large reference window of length L_1 ($L_1 \gg L$) that contains a GPS signal where the influence of the GPS signal on the accuracy of w is insignificant;
- to use a small reference window of length $L \ll L_1$ that contains a GPS signal where the maximal value is removed before estimation of the noise power.

The scale factor $T\alpha$ in (20 and 24) maintaining the required constant level of false alarm is:

$$P_{FA} = (1 + T\alpha)^{-L} \tag{27}$$

6. Performance measures

The effectiveness of the GPS MDVR CFAR algorithm for detection of the C/A code in heavy noise environment is expressed in terms of three quality measures (Fig.4). These quality measures evaluate the influence of different factors on the performance of each processing stage.

6.1 SINR improvement factor

The performance of a beamforming algorithm can be evaluated in terms of the signal-to-interference-plus-noise ratio (SINR) improvement factor estimated at the beamformer output. For a single element array the input SINR is defined as:

$$SINR_{INPUT} = \frac{P_S}{P_N + P_i} \tag{28}$$

where P_S is the average power of the desired GPS signal, P_N is the receiver noise power, and P_i is the total broadband interference power. According to the superposition principle, the SINR at the beamformer output can be evaluated as

$$SINR_{OUT} = \frac{(W^H s)(W^H s)^H}{(W^H x_0)(W^H x_0)^H} \tag{29}$$

In (29), x_0 is the total noise (noise + interference) at the antenna array element. The SINR improvement factor provided by the beamformer can be found as:

$$K_{SINR} = SINR_{OUT} / SINR_{INPUT} \tag{30}$$

As usual, this quality measure is expressed in dBs:

$$K_{SINR,dB} = SINR_{OUT,dB} - SINR_{INPUT,dB} \tag{31}$$

The SINR improvement factor evaluates the capability of the beamformer (conventional or MVDR) to cancel the interference power in the incoming signal and improve SINR at the beamformer output. If the Monte Carlo approach is used to estimate the SINR improvement factor, then the estimate of this quality measure is calculated as:

$$K_{SINR,dB} = \frac{1}{N_{total}} \sum_{n=1}^{N_{total}} K_{SINR,dB,n} \tag{32}$$

where $K_{SINR,dB,n}$ is the estimate obtained in the n-th run, and N_{total} is the total number of Monte Carlo runs.

6.2 Post correlation SNR

The detectability of the C/A code directly depends on the signal-to-noise ratio at the cross-correlator output. The impact of the circular cross-correlation algorithm is evaluated in terms of the post correlation SNR estimated at the cross-correlator output:

$$SNR_{cor} = P_{max} / SLB_{ave} \tag{33}$$

where $P_{\max}$ is the peak power at the cross-correlator output, and SLB_{ave} is the average sidelobe level. As usual, this quality measure is expressed in dBs:

$$SNR_{cor,dB} = P_{\max,dB} - SLB_{ave,dB} \tag{34}$$

If the Monte Carlo approach is used to estimate the post correlation SNR, then the estimate of this quality measure is calculated as:

$$SNR_{cor,dB} = \frac{1}{N_{total}} \sum_{n=1}^{N_{total}} SNR_{cor,dB,n} \tag{35}$$

where $SNR_{cor,dB,n}$ is the estimate obtained in the n-th cycle of simulation

6.3 Probability of detection

This quality measure evaluates the capability of the overall three-stage GPS MDVR CFAR algorithm to detect the beginning point of the C/A code and find correctly the carrier frequency of the incoming IF signal while maintaining the required probability of false alarm. This performance measure can be evaluated using the Monte Carlo approach:

$$P_D = K_{success} / N_{total} \tag{36}$$

where $K_{success}$ is the number of successful events, and N_{total} is the total number of runs.

7. Statistical analysis

7.1 Simulation algorithm

The performance of the GPS MDVR CFAR detection algorithm is evaluated using the Monte Carlo approach. The structure of the simulation algorithm is presented in Fig. 9.

The statistical estimates of the quality factors are evaluated for each stage of the detection algorithm. The goal of the Monte Carlo analysis is:

- to analyze the capability of two beamformers, non-adaptive (conventional) and adaptive (MVDR), to mitigate broadband radio frequency interference (RFI) at the navigation receiver input and as a result improve the post correlation SNR and increase the detectability of the C/A code in conditions of strong jamming;
- to evaluate the influence of several important factors on the performance of the joint three-stage detection algorithm. These factors are: interference-to-signal ratio (*ISR*); planar array configuration (*URA* and *UCA*); number of array elements (*M*); sampling rate of the incoming data (*f*s); steering vector mismatch ($\Delta\varphi, \Delta\theta$).

The simulation algorithm includes four consequential processing steps during each simulation cycle. Firstly, for each antenna element the complex valued signal is simulated in accordance with all important parameters of a GPS signal, interference and antenna array. The next processing steps include simulation of the performance of beamforming, cross-correlation and CFAR detection. For each simulation cycle, the current values of two quality measures, SINR improvement and SNR, are evaluated at the cross-correlator output by (31) and (34). If the beginning point and the carrier frequency of the C/A code are estimated correctly, then the counter $K_{success}$ in (36) is incremented by 1. When all cycles of simulation are successfully accomplished, the statistical estimates of the three quality measures are calculated by (32), (35) and (36).
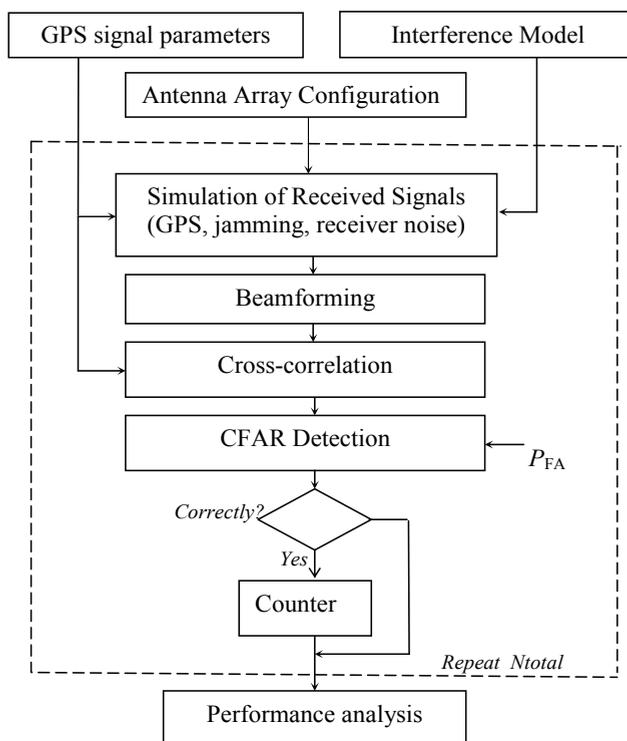
Fig. 9. Block diagram of the simulation algorithm

7.2 Simulation scenario

In this study, 1000 computer simulations of the adaptive three-stage algorithm for detection of the C/A code are performed in order to evaluate the influence of such factors as array configuration, number of array elements and sampling rate on the capability of this detection algorithm to operate effectively in conditions of strong jamming. In GPS applications, the interelement spacing in antenna arrays is approximately 0.09m for frequency L1, and this technical demand puts a physical limitation on how small the array can be used in a GPS receiver and how many elements are appropriate to be used in such an antenna array. We consider in the study two small array configurations shown in Fig. 10.

In the first antenna array (UCA-7), the first (reference) element is located at the array center but the other six elements are circular relative to the center. The second antenna array (URA-9) is rectangular and contains nine elements with half-wavelength interelement spacing. Both antenna arrays have the same overall dimensions of about 20cm. It is well known that the number of antenna elements M is related to the number of broadband jammers that can be nulled by the beamforming algorithm. Typically, the number of broadband jammers that can be nulled by the beamforming algorithm corresponds to (M-1). Taking into account the angular resolution of the two antenna arrays, the simulation scenario includes the presence of one satellite and four jamming sources located at different positions in space. The angular coordinates of both, satellite and jammers, are presented in Table 1.
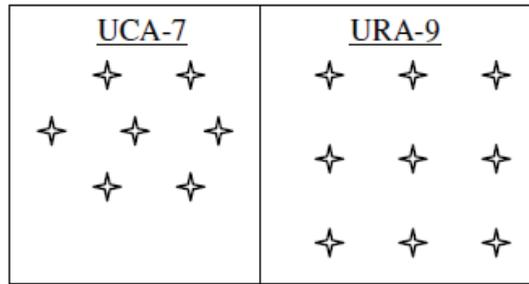
Fig. 10. Antenna array configurations used in simulations

Variant	Jamming	GPS signal
IF carrier: 1.2513 MHz Sampling: 5.0053 MHz	Four jammers: Elevation: θ=40° Azimuth:	Elevation: θ=40° Azimuth: φ=0° Doppler shift: 5 kHz
IF carrier: 2.4967 MHz Sampling: 9.9868 MHz	φ_1=-70°; φ_2=-60°; φ_3=60°; φ_4=70° ISR: 10dB … 100dB	SNR: -20dB Duration: 1ms C/A code: satellite 19

Table 1. Inteference and signal parameters

According to (10), the intensity of the signal received from a satellite is determined by the value of the signal-to-noise ratio (SNR) observed at the receiver input. In real situations, the SNR observed at the receiver input is between -15 and -30 dB. In our simulations, the SNR is assumed to be equal to -20dB. In (11), the interference intensity is determined by the value of the interference-to-noise ratio (INR) observed at the receiver input. In our case the parameter INR is expressed in terms of the interference–to-signal ratio (ISR), which describes the severity of the interference situation at the GPS receiver input.

$$INR_{dB} = ISR_{dB} + SNR_{dB} \tag{37}$$

In simulations, the parameter ISR varies between 10dB and 100 dB in increments of 5dB.

7.3 Simulation results

In broadband interference environment, the effectiveness of the GPS MDVR CFAR detection algorithm depends on the capability of the beamforming stage as much as possible to suppress interference before the cross-correlation stage. In order to compare the effectiveness of the two beamforming algorithms, the SINR improvement factor is evaluated at the output of each of the two beambormers (conventional and MVDR) as a function of the input ISR. Figure 11(a) shows that the capability of each beamformer to suppress broadband interference depends on the array geometry (URA and UCA) and the number of array elements as well (9 and 7). It can be seen that the MVDR-beamformer very successfully mitigates broadband interference even if the interference intensity becomes 100 dB over the desired GPS signal. The MVDR-beamformer is the most effective for URA-9. The results presented in Fig.11(a) confirm that in contrast to the conventional beamformer the adaptive MVDR algorithm is able to almost completely to suppress broadband interference. Because the precise angular location of the GPS satellite is not always known, it is very important to

analyze the sensitivity of each beamformer to angular errors in satellite location (in both azimuth and elevation). The sensitivity of each beamformer to angular (azimuth and elevation) errors in satellite location is shown in Fig. 11(b) for ISR=100dB. Close inspection of the results presented in Fig.11(b) reveals that in the case of the MVDR beamformer the losses in SINR due to steering vector mismatch are tolerable when angular errors are in the interval of [-15°, 15°]. However, in the conventional beamformer the losses in SINR drastically rise with increase of angular errors in satellite location.

(a)   (b)
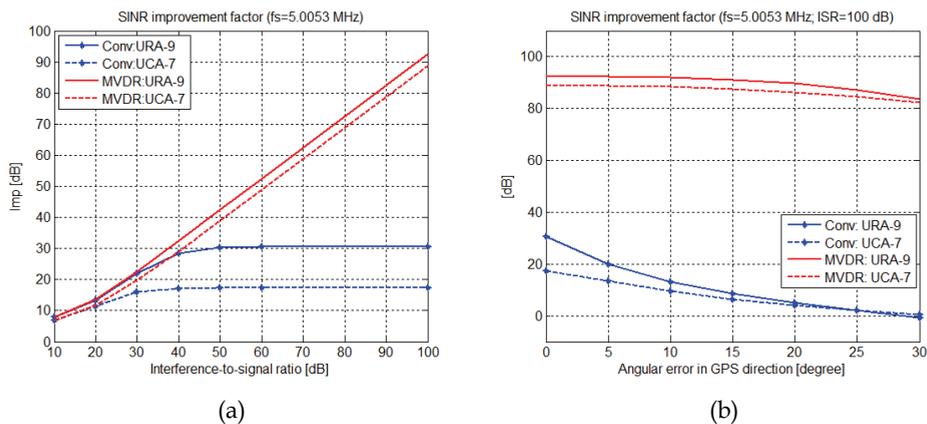
Fig. 11. SINR improvement factor as a function of ISR in case of: a)- zero angular erros , b)- nonzero angular errors in satellite position

For such a beamformer, when angular errors in satellite location equal to 5°, the SINR losses exponentially increase to the levels of 20dB – for URA-9, and 5dB – for UCA-7. The effectiveness of the first two processing blocks of the GPS MDVR CFAR detection algorithm can be expressed in terms of the SNR estimated at the cross-correlator output (Fig.12).
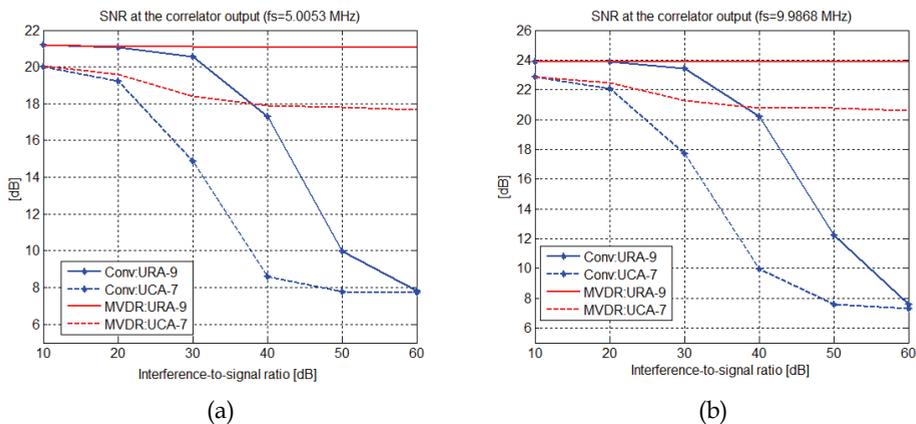

(a)   (b)

Fig. 12. SNR at the cross-correlator output as a function of ISR evaluated for two sampling frequences : (a) - fs=5.0053 MHz), (b) - fs=9.9868 MHz)

For a stable GPS signal tracking, the post correlation SNR must be at least 20 dB (Tsui, 2005). Higher post correlation SNR means the higher probability of an event in which the GPS signal is detected in the incoming signal and its both parameters, the beginning point and the carrier frequency, are correctly estimated. The results illustrated in Fig. 12 clearly show that the post correlation SNR quickly degrades with increase of the broadband interference intensity, i.e. ISR. Comparison analysis of the results from Fig. 12(a) and Fig. 12(b) shows that the post correlation SNR rises with increase of the sampling rate of the incoming data. When the sampling frequency is 10 MHz both antenna array configurations, URA-9 and UCA-7, can guarantee post correlation SNR above 20dB even if the interference intensity becomes 60 dB over the desired GPS signal. However, when the sampling frequency is 5 MHz, only URA-9 provides the SNR above 20 dB in the whole range of ISR.

The results shown in Fig. 13 demonstrate the sensitivity of the cross-correlation performance to steering vector mismatch. The results are obtained for two values of the sampling rate: Fig. 13(a) – for 5 MHz and Fig. 13(b) – for 10 MHz. The study is performed for ISR= 100 dB. It can be seen that when sampling frequency is 5 MHz, only the rectangular antenna array with 9 elements can guarantee the post correlation SNR above 20dB provided, however, that angular errors in satellite location do not exceed 15°. When the sampling frequency is doubled, both arrays can guarantee the post correlation SNR of above 20dB if angular errors in satellite location are less than 10° - for UCA-7 and less than 22° - for URA-9. These graphical results also suggest that the influence of angular errors in satellite location can be partially compensated by increasing the sampling rate of the incoming data.
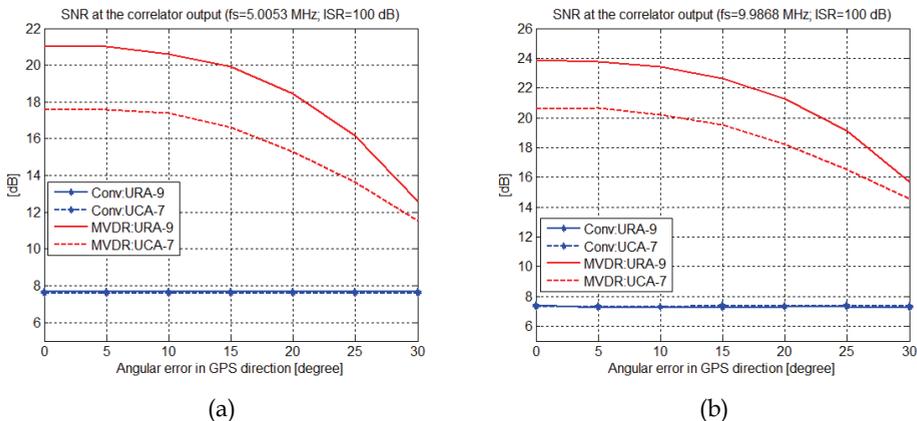

(a)   (b)

Fig. 13. SNR at the cross-correlator output as a function of angular errors evaluated for two sampling frequences : (a) - fs=5.0053 MHz), (b) - fs=9.9868 MHz)

The CFAR thresholding procedure is simulated using the modified test statistics (26). The noise level estimate w is formed using the expression (25). The scale factor T_α in (27) is determined to maintain the required probability of false alarm (P_{fa} =10[-7] and 10^{−9}). Since in real situations the presence of a GPS signal in the reference window is unknown, the objectives of the study are: (i)-to determine the minimal window of length L_1, in which the influence of the presence of a GPS signal on the accuracy of the estimate w is insignificant; (ii)- to compare two CFAR algorithms, the first of which uses the reference window of

length L_1 and the other uses the reference window of length L (L_2 << L_1) where the maximal value is removed from the reference window before estimation of the noise level. In Fig.14, the probability of detection is plotted as a function of the interference-to-signal ratio when two beamforming algorithms are used to mitigate broadband interference at the receiver input. These results are presented for different reference windows free of a GPS signal: Fig.14(a) – for the conventional beamforming algorithm and Fig.14(b) - for the MVDR. The detection probabilities are evaluated for P_{fa}= 10^{-9}. These results confirm that in case when a GPS signal is not present in the reference window, the minimal length of a reference window needed to accurately estimate the noise level is L=60. It can be seen that unlike the conventional beamformer the MVDR-beamformer successfully mitigates broadband interference and therefore the GPS MVDR CFAR detection algorithm maintains the high probability of detection within a wide diapason of the intensity of interference (ISR).
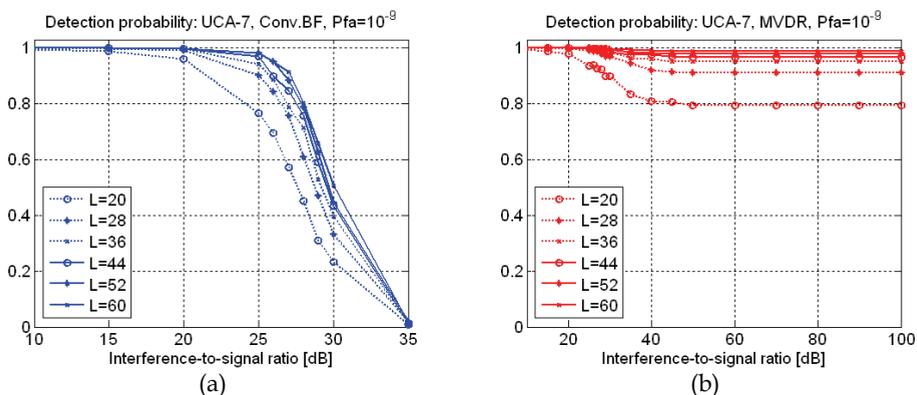
Fig. 14. Detection probability evaluated for reference windows free of a satellite signal: (a) - conventional BF ; (b) – MVDR
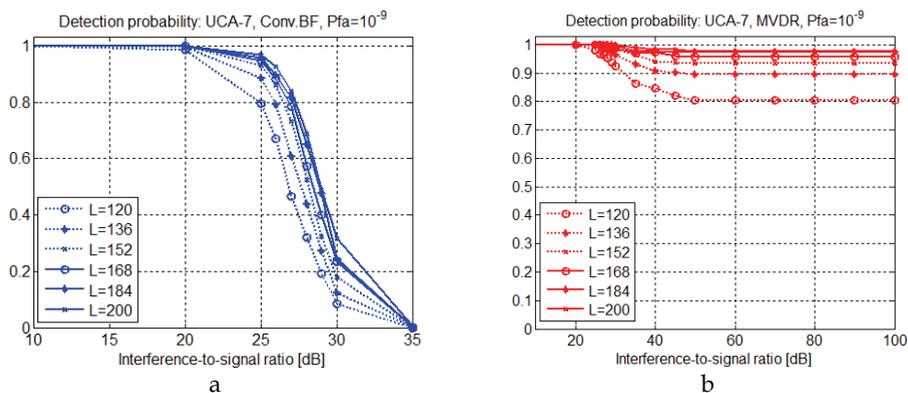

Fig. 15. Detection probability evaluated for reference windows with the GPS signal:
(a) - conventional BF; (b) – MVDR

In Fig. 15, the probability of detection is plotted as a function of ISR when the reference window used for estimation of the noise level contains a GPS signal. The reference window

length varies between 120 and 200 elements. The detection probabilities evaluated for $P_{fa}= 10^{-9}$ are shown in Fig. 15(a) - for the conventional beamforming algorithm and Fig. 15(b) - for the MVDR algorithm. It is shown that a 200-element reference window is sufficient for accurate estimation of the noise level when it contains a GPS signal (L_1=200).

The detection probabilities plotted in Fig.16 are obtained in case when a 61-element reference window that contains a GPS signal is used for estimation of the noise level. The results illustrate that this reference window can be used for estimation of the noise power if its maximal sample is previously removed before estimation (Conv.BF-OS and MVDR-OS).

(a)   (b)
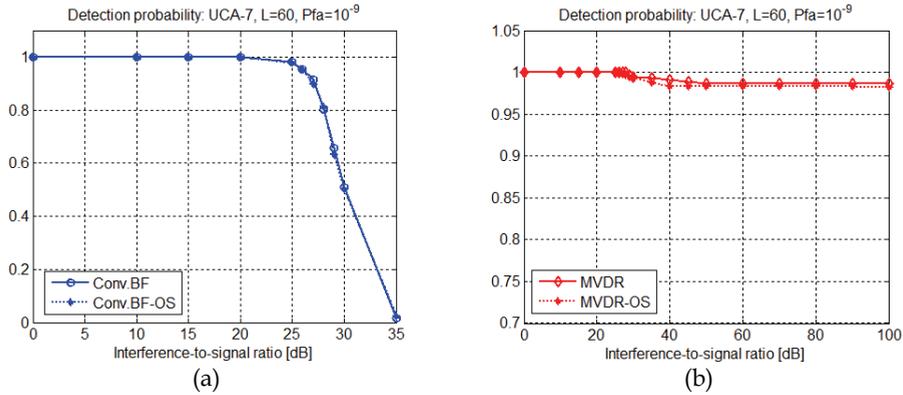
Fig. 16. Detection probability as a function of ISR evaluated for a 60-element reference window free of a GPS signal (Conv.BF and MVDR) and for a 61-element reference window containing a GPS signal (Conv.BF-OS and MVDR-OS)

The results shown in Fig. 17 demonstrate the sensitivity of the detection performance to steering vector mismatch. In Fig. 17(a), the detection probabilty is plotted for two beamforming algorithms, two values of P_{fa} and ISR=25dB. The analysis of the results shows that the probability of detection degrades with increase of angular errors in satellite location.

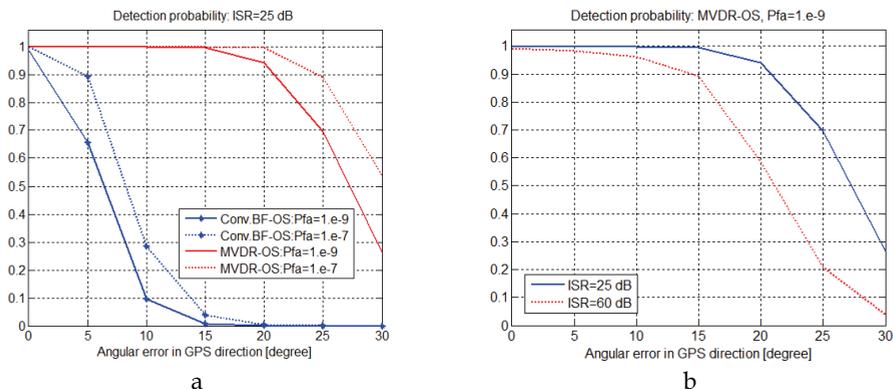a   b

Fig. 17. Detection probability as a function of angular errors evaluated for a 61-element reference window with removal of its maximal value before estimation of the noise level: a) ISR=25 dB, Pfa=10^{-7} and 10^{-9}; b) ISR=25 dB and 60 dB

The results presented in Fig. 17(b) and obtained for two values of ISR show that the detection performance becomes more sensitive to steering vector mismatch when the interference intensity increases.

Finaly, it can be concluded that the GPS MDVR CFAR detection algorithm can guarantee the detection probability of above 0.9 while maintaining the false alarm probability of 10^{-9} when angular errors in satellite location do not exceed 15°even if the interference-to-signal ratio becomes very high (60 dB).

8. Conclusion

The proposed three-stage GPS MDVR CFAR algorithm for detection of the C/A code in the incoming IF data has very good antijamming protection in a wide range of interference intensity. The obtained results reveal show that the GPS MDVR CFAR detection algorithm can guarantee the high detection probability while maintaining the required probability of false alarm even if the interference-to-signal ratio becomes very high.

9. Acknowledgment

10. References

Behar, V.; Kabakchiev, Ch. & Rohling, H. (2010). MVDR Radar Signal processing Approach for Jamming Suppression in Satellite Navigation Receivers, *Proc. of the 11-th Intern. Radar Symp. IRS-2010*, pp.134-137, ISBN 978-9955-690-18-4, Vilnius, Lithuania, June 2010.

Behar, V.; Kabakchiev, Ch. & Rohling, H. (2010). MVDR Beamformer with a CFAR Processor for Jamming Suppression in GPS Receivers, *Proc. of the Intern. Symp. on Radio Systems and Space Plasma ISRSSP'10*, pp.9-12, ISBN 978-989-8425-27-0, Sofia, Bulgaria Aug. 2010.

Behar, V.; Kabakchiev, Ch.; Gaydadjiev, G.; Kuzmanov, G. & Ganchosov, P. (2009).

Parameter Optimization of the Adaptive MVDR QR-based Beamformer for Jamming and Multipath Suppression in GPS/GLONASS Receivers, *Proc. of the 16th International Conference on Integrated Navigation Systems, ICINS'2009*, pp. 325-334, ISBN 978-5-900780-69-6, Saint-Petersburg, Russia, May, 2009.

Behar, V.; Vassileva, B. & Kabakchiev, Ch. (2010). A Simulation Tool for Analysis of MTD Algorithms Employing STAP Techniques, *Proc. of the 11-th Intern. Radar Symp. IRS-2010*, pp. 516-519, ISBN 978-9955-690-18-4, Vilnius, Lithuania, June 2010.

Behar, V.; & Kabakchiev Ch. (2009). Multiple Signal Extraction in Jamming using Adaptive Beamforming with Arbitrary Array Configurations, *Cybernetics and Information Technologies*, Vol. 9, No. 3, 2009, pp. 76-85 , ISSN: 1311-9702.

Behar V.; Kabakchiev Ch. & Doukovska, L. (2000). Adaptive CFAR PI Processor for Radar Target Detection in Pulse Jamming, *Journal of VLSI Signal Processing*, Vol. 26, 2000, pp. 383 – 396, ISSN:0922-5773.

Finn, H. & Johnson, R. (1968). Adaptive detection mode with threshold control as a function of spatially sampled clutter estimation, *RCA Review*, Vol. 29, No. 3, 1968, pp. 414-464, ISSN: 0033-6831.

Fu, Z.; Hombostel, A.; Hammesfahr, J. & Konovaltsev A. (2003). Suppression of multipath and jamming signals by GPS/Galileo applications, *GPS Solutions*, No. 6, 2003, pp. 257-264, ISSN: 1080-5370.

Ganchosov, P.; Kuzmanov, G.; Kabakchiev H.; Behar V.; Romansky, R. & Gaydadjiev G. (2009). FPGA Implementation of Modified Gram-Schmidt QR-Decomposition, *Proceedings of the 3rd HiPEAC Workshop on Reconfigurable Computing*, pp. 41-51, Paphos, Cyprus, January 2009.

Garvanov, I.; Behar V. & Kabakchiev Ch. (2003). CFAR Processors in Pulse Jamming, *LNCS*, Vol. 2542, 2003, pp. 291-298, ISSN: 0302-9743.

Ioannides, P. & Balanis, C. (2005) "Uniform circular and rectangular arrays for adaptive beamforming applications", *IEEE Trans. Antenn. Wireless Propagat. Lett.*, vol.4., 2005, pp. 351-354, ISSN: 1536-1225.

Kabakchiev, Ch.; Behar, V. & Rohling, K. (2010). Adaptive C/A Code Acquisition in Conditions of Broadband Interference with MVDR and CFAR Techniques, *Proc. of the European Navig. Conf. on Glob. Navig. Satel. Syst. - ENC GNSS 2010*, Braunschweig, Germany, Oct. 2010 (accepted).

Kabakchiev, Ch.; Rohling, H.; Garvanov, I.; Behar V. & Kyovtorov, V. (2010). Multisensor Detection in Randomly Arriving Impulse Interference using the Hough Transform, In: *Radar Technology*, Guy Kouemou (Ed.), pp. 179-204, In-Teh, ISBN: 978-3-902613-49-3), Vukovar, Croatia, 2010.

Kabakchiev, Ch.; Behar, V.; Rohling, H.; Garvanov, I.; Kyovtorov, V. & Kabakchieva, D. (2010) Analysis of Multi-Sensor Radar Detection based on the TBD-HT Approach in ECM Environment, *Proc. of the IEEE Radar Conference – RADAR'10*, pp. 651-656, ISBN 978-1-4244-5813-4, Washington DC, USA, May 2010.

Moelker, D. (1996). Adaptive antenna arrays for interference cancellation in GPS and GLONASS receivers, *Proc. of the IEEE conf. on Position Location and Navigation*, pp. 191-196, ISBN: 0-7803-3085-4, Atlanta, GA, Apr. 1996.

Sklar, J. (2003). Interference mitigation approaches for the Global Positioning System, *MIT Lincoln Laboratory Journal*, vol.14, No 2, 2003, pp. 167-177

Soubielle,J.; Fijalkow, I.; Duvau, P. & Bibaut, A. (2002). GPS positioning in a multipath environment, *IEEE Trans. on Signal Processing*, Vol. 50, No 1, 2002, pp. 141-150, ISSN: 1053587X

Tsui,J. (2005). *Fundamentals of Global Positioning System Receivers: A Software Approach*, John Wiley & Sons Inc, ISBN: 0-471-70647-7, New York

Tummonery,L.; Proudler, I.; Farina, A. & McWhirter, J. (1994). QRD-based MVDR algorithm for adaptive multi-pulse antenna array signal processing, *IEE Proc. Radar, Sonar, Navigation,* Vol. 141, No. 2, 1994, pp. 93-102, ISSN: 1350-2395.

van Trees, H. (2002). *Optimum Array Processing: Part IV of Detection, Estimation, and Modulation Theory*, JohnWiley and Sons Inc., ISBN: 978-0-471-09390-9, New York

Vouras, P. & Freburger, B. (2008). Application of adaptive beamforming techniques to HF radar, *Proc. of the IEEE conf. RADAR'08*, pp.6, ISSN: 1097-5659, Rome, Italy, May 2008
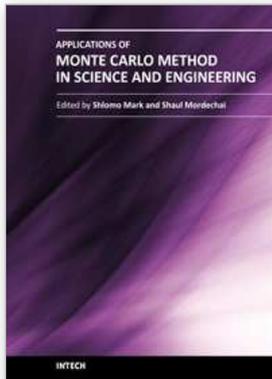
In this book, Applications of Monte Carlo Method in Science and Engineering, we further expose the broad range of applications of Monte Carlo simulation in the fields of Quantum Physics, Statistical Physics, Reliability, Medical Physics, Polycrystalline Materials, Ising Model, Chemistry, Agriculture, Food Processing, X-ray Imaging, Electron Dynamics in Doped Semiconductors, Metallurgy, Remote Sensing and much more diverse topics. The book chapters included in this volume clearly reflect the current scientific importance of Monte Carlo techniques in various fields of research.

How to reference

In order to correctly reference this scholarly work, feel free to copy and paste the following:

V. Behar, Ch. Kabakchiev, I. Garvanov and H. Rohling (2011). Performance Analysis of Adaptive GPS Signal Detection in Urban Interference Environment using the Monte Carlo Approach, Applications of Monte Carlo Method in Science and Engineering, Prof. Shaul Mordechai (Ed.), ISBN: 978-953-307-691-1, InTech, Available from: http://www.intechopen.com/books/applications-of-monte-carlo-method-in-science-and-engineering/performance-analysis-of-adaptive-gps-signal-detection-in-urban-interference-environment-using-the-mo

INTECH
open science | open minds